# Tumor invasion unit in gastric cancer revealed by QDs-based *in situ* molecular imaging and multispectral analysis☆

Wen-Qing Hu [a],[1], Min Fang [b],[1], Hao-Liang Zhao [c], Shu-Guang Yan [d], Jing-Ping Yuan [b], Chun-Wei Peng [b], Gui-Fang Yang [b], Yan Li [b],*, Jian-Ding Li [a],**

[a] Department of Medical Imaging, The First Affiliated Hospital of Shanxi Medical University, Taiyuan 030001, PR China
[b] Departments of Oncology & Pathology, Zhongnan Hospital of Wuhan University, Hubei Key Laboratory of Tumor Biological Behaviors & Hubei Cancer Clinical Study Center, Wuhan 430071, PR China
[c] Department of General Surgery, Shanxi Dayi Hospital, Taiyuan 030001, PR China
[d] Department of Surgery, Heji Hospital Affiliated to Changzhi Medical College, Changzhi 046000, PR China

## ARTICLE INFO

## ABSTRACT

In tumor tissues, cancer cells, tumor infiltrating macrophages and tumor neo-vessels in close spatial vicinity with one another form tumor invasion unit, which is a biologically important tumor microenvironment of metastasis to facilitate cancer invasion and metastasis. Establishing an *in situ* molecular imaging technology to simultaneously reveal these three components is essential for the in-depth investigation of tumor invasion unit. In this report, we have developed a computer-aided algorithm by quantum dots (QDs)-based multiplexed molecular imaging technique for such purpose. A series of studies on gastric cancer tumor tissues demonstrated that the tumor invasion unit was correlated with major unfavorable pathological features and worse clinical outcomes, which illustrated the significantly negative impacts and predictive power of tumor invasion unit on patient overall survival. This study confirmed the technical advantages of QDs-based *in situ* and simultaneous molecular imaging of key cancer molecules to gain deeper insights into the biology of cancer invasion.

## 1. Introduction

Gastric cancer (GC) is the fourth most common cancer worldwide [1], and the third leading cancer cause in China [2]. Despite recent progresses in the early diagnosis and the surgery-centered multidisciplinary treatments for GC, the overall clinical outcome of such patients is still far from satisfactory, mainly due to the post-treatment occurrence and metastasis, via blood circulation, lymphatic channels or direct cancer cells escape and seeding [3]. To tackle this problem, many efforts focusing on cancer cells have been made [4,5]. And eventually, the oncology community has come to the understanding that cancer is a disease of imbalance, *i.e.*, not merely a disease of rogue cells but the body's mismanagement of those cells, the fundamental importance of such theoretical

changes is that we have to pay particular attention to tumor microenvironment, in addition to cancer cells, because tumor microenvironment plays an important role via the co-evolution of cancer cells and stroma [3,6]. Thus, exploring the co-evolution of cancer cells and surrounding stroma is a new frontier to investigate the complex mechanisms of tumor progression.

In GC, tumor microenvironment is a complex and dynamic community, which is undergoing constant evolutions during cancer invasion, involving tumor cells escape from primary sites into vasculature (blood circulation and lymphatic channel), reside and adhere to endothelial cells, penetrate from vasculature into other organs and reside in them, accompanied with tumor neo-vessels growth [7]. Many important components in tumor microenvironment work together to contribute to cancer invasion, involving inflammatory cells such as macrophages, immune cells such as T and B lymphocytes, stromal cells such as fibroblasts, and neo-blood vessels of various stages of maturity [8]. These players must be in an appropriate anatomic proximity and spatial vicinity with the tumor cells in order to facilitate cancer invasion. And indeed, recent studies have shown that tumor cells, macrophages and tumor neo-vessels in close vicinity with one another form a unique structure called tumor microenvironment of metastasis (TMEM) [9,10], or in

more easily understandable terms, called 'tumor invasion unit' (Fig. 1). Therefore, the simultaneous recognition and analysis of all the components in the tumor invasion unit is very important to understanding the new perspective of cancer invasion.

There are few techniques that can simultaneously image multiple components in a complex tumor microenvironment of the same tissue section. Thus, it is urgent to develop a more holistic method to image the complex interactions of stromal components *in situ*. Quantum dots (QDs), with its unique size and surface effects, have shown great potential in biomedical application, especially in multiplexed imaging *in situ* [11]. In this study, taking the advantages of established QDs-based multiplexed imaging *in situ*, we analyzed on the interactions between macrophages, tumor neo-vessels and cancer cells, and developed a computer-based algorithm of tumor invasion unit.
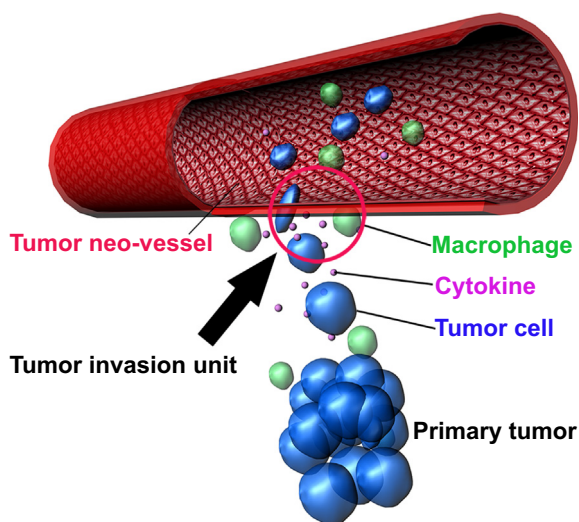
## 2. Materials and methods

### 2.1. Patients and specimens

Tissue sections (4 μm thickness) of 90 human GC cases were selected from the central database on GC established at our cancer center, including 30 with detailed pathological information, and 60 with complete clinico-pathological and survival information available on the patients. This database has been the source of information for several published studies [8,12,13]. Tumor tissues from the first set of 30 patients were used for a trial study, to explore the correlation of tumor invasion unit with classical pathological features, in order to test if there was any relationship between tumor invasion unit with unfavorable pathological features. Tumor tissues from the second set of 60 patients with detailed survival information were used for validation study, in order to further verify if tumor invasion unit could predict the overall survival (OS). The study protocol was approved by the Institutional Ethics Committee of the hospitals. Written informed consent was obtained from the patients before surgery, with permission to use the specimens for scientific research purposes, as well as clinical pathological studies.

### 2.2. QDs-based double molecular imaging

For QDs-based double molecular imaging, the primary antibodies were mouse anti-human monoclonal antibody against macrophages (MA1-38069, ABR, USA; dilution 1/300) and goat anti-human polyclonal antibody against CD105 (sc-20072, Santa Cruz, USA; dilution 1/300). The secondary antibodies were QDs-525 goat F(ab')₂ anti-mouse IgG conjugate (Invitrogen, USA; dilution 1/300, emitting green light) and QDs-655 rabbit F(ab')₂ anti-goat IgG conjugate (Invitrogen, USA; dilution 1/1000, emitting red light). The QDs-based *in situ* molecular imaging procedures were performed according to our previously established technical processes

[11,14,15], with the following major steps: tissue slides de-paraffinizing → antigen retrieval → blocking → primary antibody for macrophages and CD105 → washing and blocking → staining with QDs-525 and QDs-655 → washing → detection and acquisition. The detailed protocol was illustrated in Fig. 2A.

### 2.3. Evaluation of macrophages and tumor neo-vessels

The QDs stained images were captured by Olympus DP72 camera (Olympus Optical Co., Ltd., Tokyo, Japan) under CRi Nuance multispectral imaging system (Cambridge Research and Instrumentation, Inc., Woburn, MA, USA). The QDs-525 and QDs-655 were excited by UV light (330–385 nm). A spectral cube for each image, which contains the complete spectral information at 10 nm wavelength intervals from 420 to 720 nm, was collected by the CRi Nuance multispectral imaging system. And all the cubes were captured under the same condition at ×200 magnification with the same settings for each image, so as to avoid the selection bias (Fig. 2B). The QDs fluorescence signal unmixing was processed by the software package within the Nuance system as previously described [16]. Then, after obtaining the images of signal unmixing, the macrophages were counted on each image and the total macrophages number was documented as the counts for the patient for further analysis. The same calculation method was used for tumor neo-vessels counting (Fig. 2C–D).

### 2.4. Definition and evaluation of 'tumor invasion unit'

After processing QDs images, the images with double signals of both macrophages and tumor neo-vessels at the tumor nest area were acquired (Fig. 2B). As the tumor invasion unit consisted of tumor cells, macrophages and tumor neo-vessels, a circle with the diameter of 60 μm [9] centered on macrophages was chosen, approximately three cell diameters across. With the computer-based algorithm, if there was any red signal in this circle, it was counted as 1, otherwise; it was counted as 0. Then the total counts of five images for each patient was output as the result of tumor invasion unit (Fig. 2D).

### 2.5. Statistical analysis

Statistical analyses were performed with SPSS software version 21.0 (SPSS Inc. Chicago, IL). For the comparison of individual variables, Fisher's exact test, *t* test and Mann–Whitney Test were conducted as appropriate. The Kaplan–Meier survival curves were plotted to analyze the OS by different study parameters, with log rank test to define the statistical differences between the subgroups. Two sided $P < 0.05$ was judged as statistically significant.
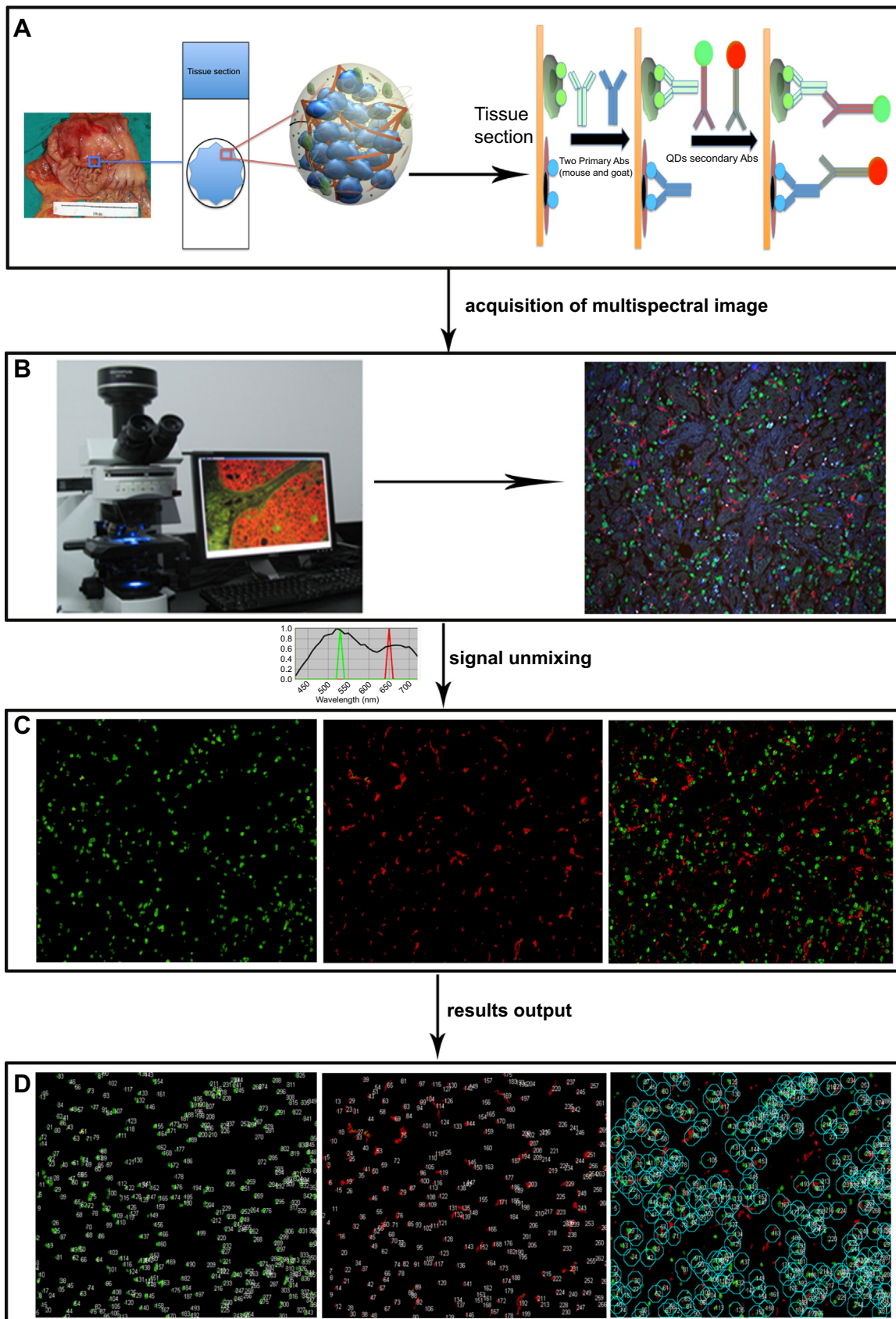
## 3. Results

### 3.1. Forms of tumor invasion unit in dynamic changes

With QDs-based *in situ* molecular imaging and multispectral analysis, the tumor infiltrating macrophages and neo-vessels were clearly marked in the easily discernable background of tumor tissue (Fig. 3). Based on the spreading and layout patterns of neo-vessels and the macrophages infiltration steps, two forms of tumor invasion unit in constant dynamic changes could be recognized. In form one (Fig. 3A1–A3), the tumor neo-vessel was seen in longitudinal section as shown in circle 1. With the special longitudinal spreading and irregular morphology, the tumor neo-vessels presented to be multi-angled accompanied with macrophages infiltration at each angle (Fig. 3A2, circle 2). Macrophages undergoing intravasation could also be observed, half in and half out of the blood vessel (Fig. 3A3, circle 3 & 4). In form two (Fig. 3B1–B3), the tumor neo-vessel is seen in cross section, with macrophages lodging the vessel with membrane processes (Fig. 3B1, circle 5), crossing the vessel wall (Fig. 3B2, circle 6), and in close vicinity to the vessel (Fig. 3B3, circle 7), thus revealing the dynamic interactions between macrophages and neo-vessels to facilitate tumor invasion.

### 3.2. Correlation of tumor invasion unit with clinico-pathological features

First, we selected a trial set of 30 GC patients with the three most common pathological types, including well differentiated, poorly differentiated and signet-ring cell carcinoma. These patients were classified into 3 groups by different pathological types, 10 cases in each group. The basic clinico-pathological characteristics



**Fig. 1.** The concept of tumor invasion unit. Tumor angiogenesis and macrophages infiltration are two important contributors to cancer invasion and metastasis. Tumor cells, macrophages and neo-vessels in close vicinity with one another form a spatially and functionally unique structure called tumor invasion unit to promote cancer cells invasion (Red circle in this illustration). (For interpretation of the references to color in this figure legend, the reader is referred to the web version of this article.)

**Fig. 2.** The QDs-based *in situ* molecular imaging and multispectral analyses of tumor invasion unit in GC. (A) Tumor slides from GC specimens were first stained with 2 primary antibodies against macrophages and CD105, a marker of tumor neo-vessels; and then stained with QDs secondary antibodies, with the macrophages stained green (525 nm spectrum) and neo-vessels stained red (655 nm spectrum). (B, C) The images were computer captured and unmixed by multispectral analysis software, to delete the signal noise and set the spectral images of macrophages and neo-vessels for subsequent analysis. (D) With green signal of a macrophage as the center, a 60 μm-diameter circle was set to see if there were any red signals of neo-vessels in this circle. Only circles with both macrophage and neo-vessel signals were considered as tumor invasion units. The total number of circles was counted as the final output results of tumor invasion unit. GC: gastric cancer. (For interpretation of the references to color in this figure legend, the reader is referred to the web version of this article.)
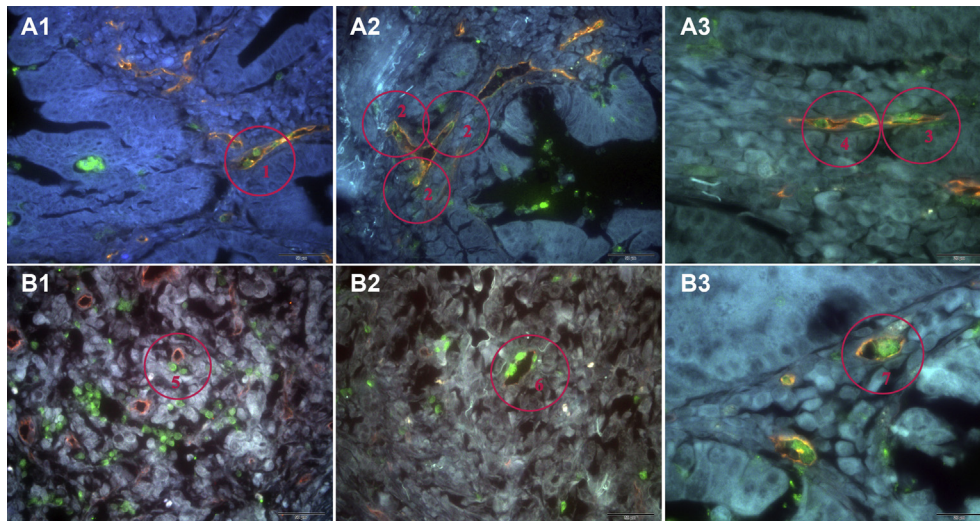
**Fig. 3.** Two forms of tumor invasion unit. With QDs-based *in situ* molecular imaging technique, various forms of neo-vessels and macrophages infiltration could be clearly demonstrated in the easily discernable background of cancer tissue. Two forms of tumor invasion unit were observed. In tumor invasion unit form one (A1-A3), the neo-vessels were in longitudinal spreading and multi-angle form, frequently accompanied with macrophages attaching to the vessel wall (circle 1), and infiltrating the tumor tissue at the angles (circle 2). In some circumstances, the entire process of macrophages infiltration could be observed, from lodgment and attachment to neo-vessels (circle 3) to penetration of the blood vessel showing an interesting phenomenon of macrophage half in and half out of the neo-vessel (circle 4). In tumor invasion unit form two (B1–B3), neo-vessels are in cross section, with macrophages lodging the vessel with membrane processes (circle 5), crossing the vessel wall (circle 6), and in close vicinity to the vessel (circle 7), thus revealing the dynamic interactions between macrophages and neo-vessels to facilitate cancer invasion. Macrophages: green; Neo-vessels: red; Tumor tissue background: gray or blue. Scale bar = 50 μm for A1, A2, B2 & B3; = 20 μm for A3 & B1. (For interpretation of the references to color in this figure legend, the reader is referred to the web version of this article.)

including age at diagnosis, sex, tumor size, tumor invasion depth, and lymph node metastases were statistically not significant among the three groups (Table 1). The QDs-stained slides from each patient were quantitatively analyzed for neo-vessels and macrophages density. According to the quantitative analysis results, the median value of macrophages density was higher in the poorly differentiated group (1544) than the well differentiated group (317) and the signet-ring cell group (1011), with statistical significance in three groups ($P = 0.001$, for between-group comparisons). The results of tumor neo-vessels analysis were the same as the macrophages. The poorly differentiated group had the highest count but the well differentiated group had the lowest count, with statistical significance among three groups ($P = 0.029$, for between-group comparisons). And also, the number of tumor invasion unit was much higher in the poorly differentiated group (373) than the well differentiated group (82) or the signet-ring cell group (177), with statistical significance in three groups ($P = 0.000$, for between-group comparisons). Thus, in this trial set, compared with the analysis results of macrophages and tumor neo-vessels, tumor invasion units had the similar effects. However, the $P$ value of tumor invasion unit was the smallest, suggesting its stronger correlation with worst histological types.

### 3.3. Impact of tumor invasion unit on clinical outcome

As the above study demonstrated that tumor invasion unit could be a more important parameter with worse histological features, we conducted a validation study in 60 GC patients with known clinical outcomes. Taking the median value of macrophages, neo-vessels density and tumor invasion unit as the cut-off value, these 60 GC patients were divided into high density group if the individual value was above the cut-off value, and low density group if the individual value was below the cut-off value. The major clinico-pathological features of these patients were listed in Table 2, and their OS curves by macrophages density (Fig. 4A), tumor neo-vessels density (Fig. 4B) and tumor invasion unit (Fig. 4C) showed that both macrophages density and tumor invasion unit were independent factors to impact on OS, while tumor neo-vessels density itself was not an independent factor for OS. ROC analysis also demonstrated that tumor invasion unit had the largest area under the curve (63.2%), suggesting that tumor invasion unit had bigger predicting power than macrophages for OS prediction (Fig. 4D).

**Table 1**
Major demographic and clinico-pathologic characteristics of 30 GC patients in the trial study.

| Items | Major histological types | | | P Value |
|---|---|---|---|---|
| | Well differentiated | Poorly differentiated | Signet-ring cell | |
| Number | 10 | 10 | 10 | |
| Age (yr, Mean ± SD) | 67.7 ± 9.6 | 61.4 ± 9.4 | 63.2 ± 9.9 | 0.335 |
| Sex | | | | |
| Male | 7 (70%) | 8 (80%) | 5 (50%) | 0.350 |
| Female | 3 (30%) | 2 (20%) | 5 (50%) | |
| Tumor size (cm) | | | | |
| < 2 | 2 (20%) | 0 (0%) | 1 (10%) | 0.329 |
| ≥2 | 8 (80%) | 10 (100%) | 9 (90%) | |
| Tumor invasion depth (T stage) | | | | |
| < 4 (tumor invasion not to serosa) | 3 (30%) | 0 (0%) | 1 (10%) | 0.133 |
| ≥4 (tumor invasion beyond serosa or to adjacent structures) | 7 (70%) | 10 (100%) | 9 (90%) | |
| Lymph node metastasis | | | | |
| No | 5 (50%) | 4 (40%) | 4 (40%) | 0.873 |
| Yes | 5 (50%) | 6 (60%) | 6 (60%) | |
| Macrophages density (Median, range)[a] | 317 (120−1508) | 1544 (427−3294) | 1011 (613−2394) | **0.001** |
| Tumor neo-vessels density (Median, range)[a] | 474 (244−834) | 789 (574−1228) | 774 (380−1206) | **0.029** |
| Tumor invasion unit (Median, range)[a] | 82 (0−206) | 373 (108−2011) | 177 (107−1500) | **0.000** |

[a] For the measurement of macrophages density, tumor neo-vessels density and tumor invasion unit: total counts in 5 digital images of the same tissue section at ×200 magnification were taken as the final results output.

**Table 2**
Major demographic and clinico-pathologic characteristics of 60 GC patients in the validation study.

| Items | Value |
| --- | --- |
| Age (yr, Mean ± SD) | 60.7 ± 11.6 |
| Sex | |
|   Male | 41 (68.3%) |
|   Female | 19 (31.7%) |
| Pathological types | |
|   Well differentiated | 20 (33.3%) |
|   Poorly differentiated | 23 (38.3%) |
|   Signet-ring cell carcinoma | 17 (28.3%) |
| Tumor invasion depth (T stage) | |
|   <4 (tumor invades not to serosa) | 14 (23.3%) |
|   ≥4 (tumor invades serosa or adjacent structures) | 46 (76.7%) |
| Lymph node metastasis | |
|   No | 18 (30%) |
|   Yes | 42 (70%) |
| Distant metastasis | |
|   No | 53 (88.3%) |
|   Yes | 7 (11.7%) |
| TNM stages | |
|   Early (Stage I, II) | 21 (35%) |
|   Advanced (Stage III, IV) | 39 (65%) |
| Surgery | |
|   Subtotal resection | 50 (83.3%) |
|   Total resection | 10 (16.7%) |
| Chemotherapy | |
|   No | 20 (33.3%) |
|   Yes | 40 (66.7%) |
| OS, months (Median, range) | 17.8 (1.2–46.0) |

### 3.4. Typical examples of impacts of tumor invasion unit on prognosis

From the above analysis, we have found that tumor invasion unit may have significant effects on clinical outcome. To further validate this observation, we selected 6 cases for detailed analysis (Fig. 5), 3 cases of poorly differentiated adenocarcinoma with identical TNM stages and clinical treatments (Fig. 5A–C), and another 3 cases of highly differentiated adenocarcinoma with identical TNM stages and clinical treatments (Fig. 5D–F). From these cases, it could be observed more clearly that the higher the number of tumor invasion unit, the shorter the OS was, regardless of the tumor differentiation and histological types. In the 3 cases of poorly differentiated adenocarcinoma, the tumor invasion units were 7, 20 and 58 per ×200 magnification field, respectively; and the corresponding OS were 20.6, 11.1 and 3.3 months, respectively. In another 3 cases of well differentiated adenocarcinoma, the tumor invasion units were 3, 11, and 24 per ×200 magnification field, respectively; and the corresponding OS were 42.6, 27.6, and 14.3 months, respectively.

## 4. Discussion

This study demonstrated that the complex and constant interactions between tumor cells and their microenvironment could have a significant impact on the clinical outcomes of GC patients. Specifically, tumor cells, new blood vessels due to tumor angiogenesis and infiltrating macrophages in the tumor microenvironment could form a spatially very close entity called tumor invasion unit that facilitates tumor invasion. The number of tumor invasion unit in cancer tissue is correlated with poor tumor differentiation and worse survival. In addition, the tumor invasion unit has bigger predictive power of OS than single component count of macrophages and tumor neo-vessels, respectively. More interestingly, we have found that the tumor neo-vessels density was not an independent prognostic factor for OS. This may suggest that the

effects of tumor neo-vessels on cancer invasion can be regulated by tumor macrophages infiltration with synergistic effect, by a mechanism of secreting factors, such as vascular endothelial growth factor (VEGF) to facilitate tumor angiogenesis [17,18]. This could at least account for the emerging concept of the tumor invasion unit.

There have also been several studies to explore the biological, pathological and clinical significance of tumor invasion unit. In a study by Robinson [9], the TMEM in human breast carcinoma, i.e., in our study called the tumor invasion unit, could predict the development of systematic, hematogenous dissemination. And the ability of tumor invasion unit to predict distant metastasis was independent of lymph node status and other currently used prognosticators. Further, it demonstrated that for every 10 increase in tumor invasion unit, the odds ratio for systematic metastasis was 1.9 (95% confidence interval, 1.1–3.4). And also in the mouse models researches [10,19], high-resolution two-photon imaging of the interactions between perivascular macrophages and cancer cells during intravasation has revealed the presence of tumor invasion unit that defines the site where intravasation by motile cancer cells occurs. The concept of tumor invasion unit is also similar with the emerging concept of pre-metastatic niche at distant organ area [20,21], in which tumor cells, macrophages and tumor neo-vessels together create a spatially well-arranged environment favoring cancer invasion and metastatic self-seeding [22,23].

Tumor inflammation and tumor angiogenesis are considered indispensable for cancer invasion [3]. Macrophages constitute a significant proportion of inflammatory cells and are important bridge girder between inflammation and cancer [24]. However, there is still evidence demonstrating that macrophages can exert dual impacts on cancer depending on the activation state, with classically activated (M1) and alternatively activated (M2) cells generally exerting anti-tumoral and pro-tumoral functions, respectively [25]. Thus, studies of functions of macrophages on GC are insufficient. Meanwhile, due to its pivotal role in tumor angiogenesis, macrophages have attracted considerable attention [8], involving promoting both endothelial cells to form structures of blood vessels [18] and blood vessels budding out [17]. In addition, angiogenesis is also regarded as an important hallmark of cancer, as tumor must depend on vessels to acquire nutrients and remove metabolic wastes [26]. And tumor neo-vessels characterized by the irregular morphology, structure disorder and leakiness so as to facilitate the cancer cells spread [27,28]. However, compared with these studies, when we look at all these components together, the results were more suggestive of an association with the worse clinical outcome.

The above mentioned studies of multi-component imaging in situ used conventional imaging techniques, including fluorescent dyes and double immunohistochemistry staining, to reveal the morphological features of tumor invasion unit [9]. While one component of the unit could be observed directly at one time, there must be several repeating imaging procedures to produce the overlay images, so as to reveal the intimate relationship between tumor cells, macrophages and neo-vessels. The shortcoming of these conventional techniques is that subtle by essential information on the interactions of the major components of tumor invasion unit could not be obtained simultaneously, thus leading to information loss and low resolution of different components in situ [29]. To solve this problem, there is an urgent need to develop a new technology that could simultaneously image the major components of tumor invasion unit.

QDs-based molecular imaging and multispectral analysis could make a unique contribution in this regard, as the current study demonstrated. QDs are engineered nanoparticles with unique optical properties suitable for biomedical application. Compared with
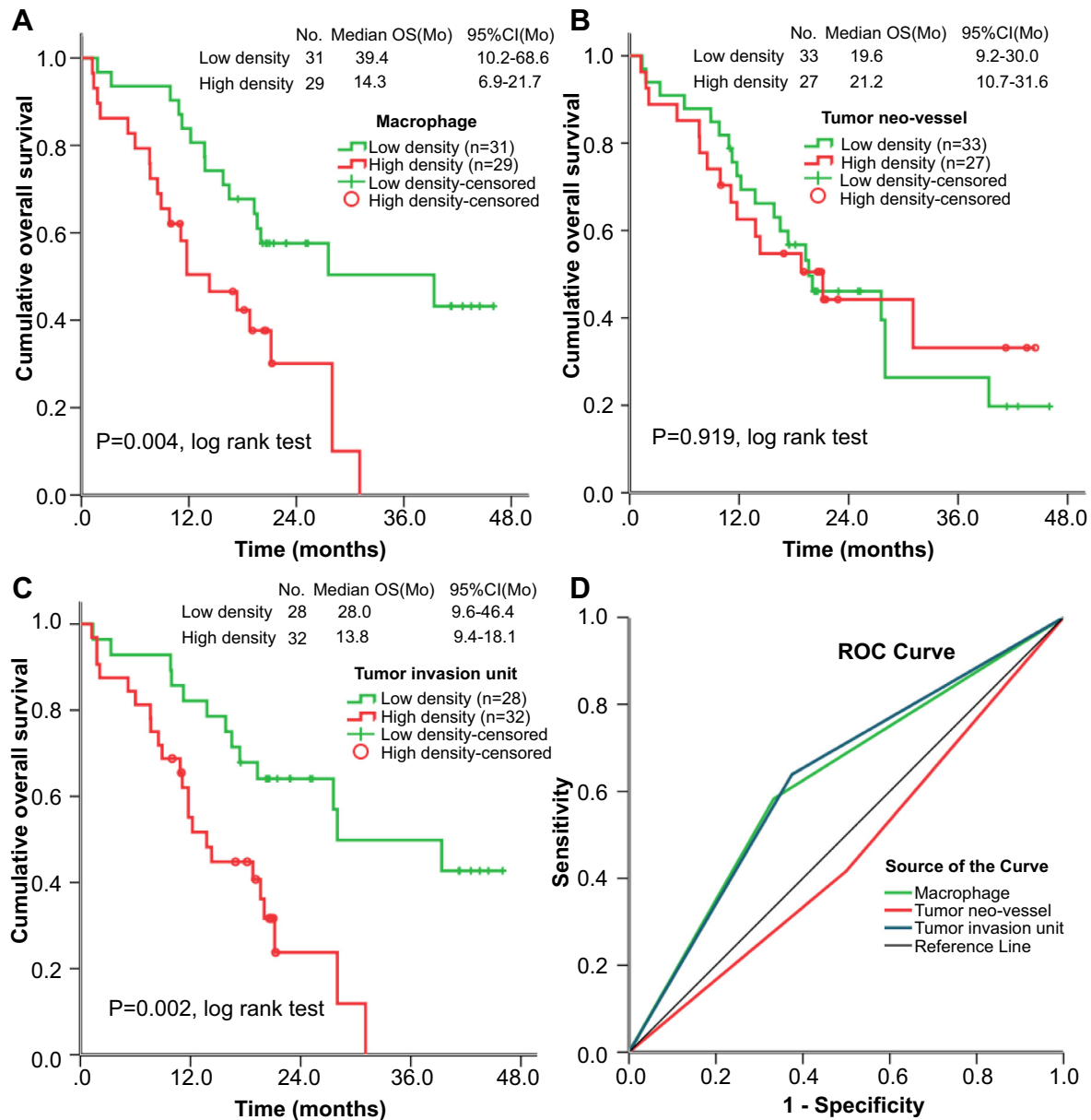
**Fig. 4.** The cumulative curves and ROC analysis. (A–C) The cumulative OS curves by macrophage, tumor neo-vessel density and tumor invasion unit, respectively. While macrophages density and tumor invasion unit could differentiate survival differences, tumor neo-vessels density was not an independent factor to differentiate survival. (D) ROC analysis of macrophages, tumor neo-vessels density and tumor invasion unit showed that tumor invasion unit had the largest area under the curve, suggesting the tumor invasion unit had better performance in predicting OS than other parameters. OS: overall survival; Mo: months.

organic dyes and fluorescent proteins, due to its unique size and surface features, QDs have many advantages such as composition-tunable light emission, enhanced fluorescence brightness, strong resistance to photobleaching and chemical degradation. In addition, different colors of QDs can be simultaneously excited by a single light source, with minimal spectral overlapping, which provides significant advantages for multiplexed detection of targets [30]. This property is very suitable for investigating the complex interactions between tumor cells and their surrounding microenvironment at the architectural level. In this study, the infiltrating macrophages and tumor angiogenesis were simultaneously labeled green and red, respectively. The blue auto-fluorescence also showed clear tumor background structure. Therefore, instead of producing artificial overlay images by conventional imaging

techniques, this QDs-based molecular imaging technique could provide authentic multicolor images to better reveal the complex interactions of different components in cancer tissues.

## 5. Conclusion

Cancer recurrence and metastasis is the root cause of treatment failure in GC, and tumor cells invasion is the first and most important step towards distant metastasis. There are currently no suitable methodologies to predict the risk of metastasis. Taking the advantages of QDs-based multiplexed molecular imaging technology, this study has simultaneously revealed the spatial distribution of tumor invasion unit, consisting of tumor cells, macrophages and tumor neo-vessels, and developed a computer-based algorithm to
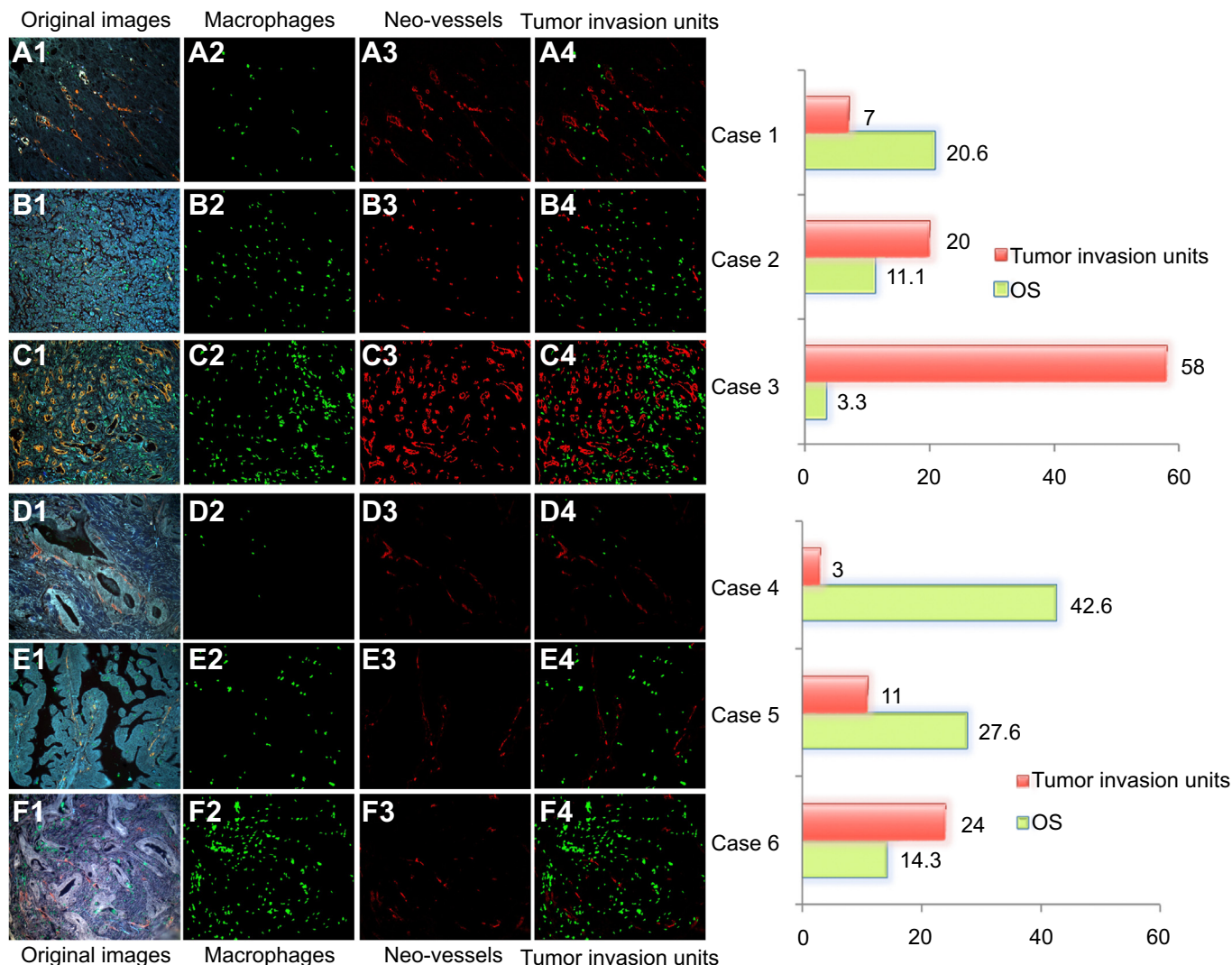
**Fig. 5.** Typical examples of negative correlation between the number of tumor invasion unit and the OS of GC patients. In 3 cases of poorly differentiated adenocarcinoma (panels A, B and C) and another 3 cases of highly differentiated adenocarcinoma (panels D, E and F) of the same TNM stage and treatments, tumor invasion unit was negatively correlated with OS of each patient. The right two graphs were the number of tumor invasion unit and the corresponding OS of each patient. Scale bar = 50 μm for A1-F4; OS: overall survival (months); the number of tumor invasion unit was the count per ×200 magnification field.

analyze tumor invasion unit at molecular level. Both the new approach and the results in this study suggest the predictive power of tumor invasion unit for OS. This research once again demonstrated the advantages of QDs-based multiplexed molecular imaging in simultaneously study several related parameters *in situ*. Future studies in a larger, independent and standardized GC database with known clinical outcome could further substantiate the practical utility of such technology.

## Disclosures

The authors report no conflicts of interest in this work.

## Acknowledgments

## References

[1] Jemal A, Bray F, Center MM, Ferlay J, Ward E, Forman D. Global cancer statistics. CA Cancer J Clin 2011;61:69—90.
[2] Chen W, Zheng R, Zhang S, Zhao P, Li G, Wu L, et al. The incidences and mortalities of major cancers in China, 2009. Chin J Cancer 2013;32:106—12.
[3] Hanahan D, Weinberg Robert A. Hallmarks of cancer: the next generation. Cell 2011;144:646—74.
[4] Gerlinger M, Rowan AJ, Horswell S, Larkin J, Endesfelder D, Gronroos E, et al. Intratumor heterogeneity and branched evolution revealed by multiregion sequencing. N Engl J Med 2012;366:883—92.
[5] Rosner M, Hengstschlager M. Targeting epigenetic readers in cancer. N Engl J Med 2012;367:1764—5.
[6] Page-McCaw A, Ewald AJ, Werb Z. Matrix metalloproteinases and the regulation of tissue remodelling. Nat Rev Mol Cell Biol 2007;8:221—33.
[7] Yasui W, Oue N, Aung PP, Matsumura S, Shutoh M, Nakayama H. Molecular-pathological prognostic factors of gastric cancer: a review. Gastric Cancer 2005;8:86—94.
[8] Peng CW, Tian Q, Yang GF, Fang M, Zhang ZL, Peng J, et al. Quantum-dots based simultaneous detection of multiple biomarkers of tumor stromal features to predict clinical outcomes in gastric cancer. Biomaterials 2012;33:5742—52.
[9] Robinson BD, Sica GL, Liu YF, Rohan TE, Gertler FB, Condeelis JS, et al. Tumor microenvironment of metastasis in human breast carcinoma: a potential prognostic marker linked to hematogenous dissemination. Clin Cancer Res 2009;15:2433—41.

W.-Q. Hu et al. / Biomaterials 35 (2014) 4125–4132



[10] Wyckoff JB, Wang Y, Lin EY, Li JF, Goswami S, Stanley ER, et al. Direct visualization of macrophage-assisted tumor cell intravasation in mammary tumors. Cancer Res 2007;67:2649–56.
[11] Fang M, Yuan JP, Peng CW, Pang DW, Li Y. Quantum dots-based in situ molecular imaging of dynamic changes of collagen IV during cancer invasion. Biomaterials 2013;34:8708–17.
[12] Peng CW, Wang LW, Zeng WJ, Yang XJ, Li Y. Evaluation of the staging systems for gastric cancer. J Surg Oncol 2013;108:93–105.
[13] Peng CW, Wang LW, Fang M, Yang GF, Li Y, Pang DW. Combined features based on MT1-MMP expression, CD11b + immunocytes density and LNR predict clinical outcomes of gastric cancer. J Transl Med 2013;11:153.
[14] Peng CW, Liu XL, Liu X, Li Y. Co-evolution of cancer microenvironment reveals distinctive patterns of gastric cancer invasion: laboratory evidence and clinical significance. J Transl Med 2010;8:101.
[15] Chen C, Sun SR, Gong YP, Qi CB, Peng CW, Yang XQ, et al. Quantum dots-based molecular classification of breast cancer by quantitative spectroanalysis of hormone receptors and HER2. Biomaterials 2011;32:7592–9.
[16] Taylor CR, Levenson RM. Quantification of immunohistochemistry–issues concerning methods, utility and semiquantitative assessment II. Histopathology 2006;49:411–24.
[17] Fantin A, Vieira JM, Gestri G, Denti L, Schwarz Q, Prykhozhij S, et al. Tissue macrophages act as cellular chaperones for vascular anastomosis downstream of VEGF-mediated endothelial tip cell induction. Blood 2010;116:829–40.
[18] Stockmann C, Doedens A, Weidemann A, Zhang N, Takeda N, Greenberg JI, et al. Deletion of vascular endothelial growth factor in myeloid cells accelerates tumorigenesis. Nature 2008;456:814–8.
[19] Wyckoff J, Wang W, Lin EY, Wang Y, Pixley F, Stanley ER, et al. A paracrine loop between tumor cells and macrophages is required for tumor cell migration in mammary tumors. Cancer Res 2004;64:7022–9.
[20] Psaila B, Lyden D. The metastatic niche: adapting the foreign soil. Nat Rev Cancer 2009;9:285–93.
[21] Kaplan RN, Riba RD, Zacharoulis S, Bramley AH, Vincent L, Costa C, et al. VEGFR1-positive haematopoietic bone marrow progenitors initiate the pre-metastatic niche. Nature 2005;438:820–7.
[22] Comen E, Norton L, Massague J. Clinical implications of cancer self-seeding. Nat Rev Clin Oncol 2011;8:369–77.
[23] Kim MY, Oskarsson T, Acharyya S, Nguyen DX, Zhang XH, Norton L, et al. Tumor self-seeding by circulating cancer cells. Cell 2009;139:1315–26.
[24] Liu Q, Zhang A, Xu W, Dong J. A new view of the roles of blood flow dynamics and Kupffer cell in intra-hepatic metastasis of hepatocellular carcinoma. Med Hypotheses 2011;77:87–90.
[25] Mantovani A, Locati M. Tumor-associated macrophages as a paradigm of macrophage plasticity, diversity, and polarization: lessons and open questions. Arterioscler Thromb Vasc Biol 2013;33:1478–83.
[26] Kerbel RS. Tumor angiogenesis. N Engl J Med 2008;358:2039–49.
[27] Rolny C, Mazzone M, Tugues S, Laoui D, Johansson I, Coulon C, et al. HRG inhibits tumor growth and metastasis by inducing macrophage polarization and vessel normalization through downregulation of PlGF. Cancer Cell 2011;19:31–44.
[28] Sethi N, Kang Y. Unravelling the complexity of metastasis–molecular understanding and targeted therapies. Nat Rev Cancer 2011;11:735–48.
[29] Kairdolf BA, Smith AM, Stokes TH, Wang MD, Young AN, Nie S. Semiconductor quantum dots for bioimaging and biodiagnostic applications. Annu Rev Anal Chem (Palo Alto Calif) 2013;6:143–62.
[30] Chen C, Peng J, Sun SR, Peng CW, Li Y, Pang DW. Tapping the potential of quantum dots for personalized oncology: current status and future perspectives. Nanomedicine (Lond) 2012;7:411–28.